Polarization insensitive all-optical wavelength conversion of polarization multiplexed signals using co-polarized pumps

Aravind P. Anthur,[1,*] **Rui Zhou,**[1] **Sean O'Duill,**[1] **Anthony J. Walsh,**[1] **Eamonn Martin,**[1] **Deepa Venkitesh,**[2] **and Liam P. Barry**[1]

[1]*School of Electronic Engineering, Dublin City University, Dublin 9, Ireland*
[2]*Department of Electrical Engineering, Indian Institute of Technology Madras, India*
[*]*aravind.p.a@gmail.com*

Abstract: We study and experimentally validate the vector theory of four-wave mixing (FWM) in semiconductor optical amplifiers (SOA). We use the vector theory of FWM to design a polarization insensitive all-optical wavelength converter, suitable for advanced modulation formats, using non-degenerate FWM in SOAs and parallelly polarized pumps. We demonstrate the wavelength conversion of polarization-multiplexed (PM)-QPSK, PM-16QAM and a Nyquist WDM super-channel modulated with PM-QPSK signals at a baud rate of 12.5 GBaud, with total data rates of 50 Gbps, 100 Gbps and 200 Gbps respectively.

OCIS codes: (190.4380) Nonlinear optics, four-wave mixing; (190.0190) Nonlinear optics.

References and links

1. P. J. Winzer, "Scaling optical fiber networks: challenges and solutions," Opt. Photon. News **26**(3), 28–35 (2015).
2. Cisco Visual Networking Index: Global Mobile Data Traffic Forecast Update, 2015–2020, February 3 (2016).
3. https://www.alcatel-lucent.com/solutions/agile-optical-networking/components.
4. M. Bhopalwala, H. Rastegarfar, D. C. Kilper, M. Wang, and K. Bergman, "Energy efficiency of optical grooming of QAM optical transmission channels," Opt. Express **24**, 2749–2764 (2016).
5. J. M. H. Elmirghani and H. T. Mouftah, "All-optical wavelength conversion: technologies and applications in DWDM networks," IEEE Commun. Mag. **38**(3), 86–92 (2000).
6. A. P. Anthur, R. T. Watts, K. Shi, J. O Carroll, D. Venkitesh, and L. P. Barry , "Dual correlated pumping scheme for phase noise preservation in all-optical wavelength conversion," Opt. Express **21**, 15568–15579 (2013).
7. A. P. Anthur, R. T. Watts, R. Zhou, P. Anandarajah, D. Venkitesh, L. P. Barry, "Penalty-free wavelength conversion with variable channel separation using gain-switched comb source," Opt. Commun. **324**, 69–72 (2014).
8. S. P. O' Duill, S. T. Naimi, A. P. Anthur, T. N. Huynh, D. Venkitesh, L. P. Barry, "Simulations of an OSNR-limited all-optical wavelength conversion scheme," IEEE Photon. Technol. Lett. **25**, 2311–2314 (2013).
9. A. P. Anthur, R. T. Watts, S. ODuill, R. Zhou, D. Venkitesh, and L. P. Barry, "Impact of nonlinear phase noise on all-optical wavelength conversion of 10.7-GBaud QPSK data using dual correlated pumps," IEEE J. Quantum Electron. **51**, 9100105 (2015).
10. S. T. Naimi, S. O'Duill and L. P. Barry,"All optical wavelength conversion of Nyquist-WDM superchannels using FWM in SOAs," J. Lightwave Technol. **33**, 3959–3967 (2015).
11. C. Li, M. Luo, Z. He, H. Li, J. Xu, S. You, Q. Yang, and S. Yu, "Phase noise canceled polarization-insensitive all-optical wavelength conversion of 557-Gb/s PDM-OFDM signal using coherent dual-pump," J. Lightwave Technol. **33**, 2848–2854 (2015).
12. T. Ito, N. Yoshimoto, K. Magari, K. Kishi, and Y. Kondo, "Extremely low power consumption semiconductor optical amplier gate for WDM applications," Electron. Lett. **33**, 1791–1792 (1997).

#261322 Received 18 Mar 2016; revised 27 Apr 2016; accepted 12 May 2016; published 20 May 2016

13. G. P. Agrawal, "Population pulsations and nondegenerate four-wave mixing in semiconductor lasers and amplifiers," J. Opt. Soc. Am. B **5**, 147–159 (1988).
14. K. Inoue, "Polarization independent wavelength conversion using fiber four-wave mixing with two orthogonal pump lights of different frequencies," J. Lightwave Technol. **12**, 1916–1920 (1994).
15. H. Zhou, J. Yu, J. Tang, L. Chen, "Polarization insensitive wavelength conversion for polarization multiplexing non-return-to-zero quadrature phase shift keying signals based on four-wave mixing in a semiconductor optical amplifier using digital coherent detection," Opt. Eng. **52**, 025001 (2013).
16. J. Lu, Z. Dong, L. Chen, J. Yu, "Polarization insensitive wavelength conversion based on four-wave mixing for polarization multiplexing signal in high-nonlinear fiber," Opt. Commun. **282**, 1274–1280 (2009).
17. Q. Lin and G. P. Agrawal, "Vector theory of four-wave mixing: polarization effects in fiber-optic parametric amplifiers," J. Opt. Soc. Am. B **21**, 1216–1224 (2004).
18. R. Zhou,T. N. Huynh, V. Vujicic, P. M. Anandarajah, and L. P. Barry, "Phase noise analysis of injected gain switched comb source for coherent communications," Opt. Express **22**, 8120–8125 (2014).
19. S. P. O Duill, P. M. Anandarajah, R. Zhou and L. P. Barry, "Numerical investigation into the injection-locking phenomena of gain switched lasers for optical frequency comb generation," Appl. Phys. Lett. **106**, 211105 (2015).
20. P. P. Baveja, D. N. Maywar and G. P. Agrawal, "Interband four-wave mixing in semiconductor optical amplifiers with ASE-enhanced gain recovery," IEEE J. Sel. Top. Quantum Electron. **8**, 899–908 (2012).
21. K. Kikuchi, "Performance analyses of polarization demultiplexing based on constant-modulus algorithm in digital coherent optical receivers," Opt. Express **19**, 9868–9980 (2011).
22. A. Leven, N. Kaneda and Y. Chen, "A real-time CMA-based 10 Gb/s polarization demultiplexing coherent receiver implemented in an FPGA," in Proceedings of OFC/NFOEC (2008), paper OTuO2.
23. Y. Mori, C. Zhang, K. Igarashi, K. Katoh, and K. Kikuchi, "Unrepeated 200-km transmission of 40-Gbit/s 16-QAM signals using digital coherent receiver, Opt. Express **17**, 1435–1441 (2009).
24. T. N. Huynh, F. Smyth, L. Nguyen, and L. P. Barry, "Effects of phase noise of monolithic tunable laser on coherent communication systems," Opt. Express **20**, B244–B249 (2012).
25. B. Filion, An. T. Nguyen, L. A. Rusch and S. LaRochelle, "Digital post-compensation of nonlinear distortions in wavelength conversion based on four-wave mixing in a semiconductor optical amplifier," J. Lightwave Technol. **33**, 3254–3264 (2015).
26. J. Gong, J. Xu, M. Luo, X. Li, Y. Qiu, Q. Yang, X. Zhang, and S. Yu, "All-optical wavelength conversion for mode division multiplexed superchannels," Opt. Express **24**, 8926–8939 (2016).

1. Introduction

Cloud computing, Internet of Things and video streaming will be driving the bandwidth requirements in the access, metro and long haul optical communication links higher [1]. As per the Cisco virtual mobile forecast, the amount of mobile generated traffic of communication networks is exponentially increasing, with the number of mobile devices connected to the internet exceeding the total world population [2]. In order to address these bandwidth requirements, the fiber connectivity will move closer to the end-user thereby increasing the back-haul traffic proportionately. In such an increasingly complex network, it will be difficult to maintain the wavelength continuity from end to end, especially when there are multiple-degree reconfigurable optical add-drop multiplexer (ROADM) nodes enroute [3]. Thus, agility in the network has become essential and a significant amount of research is focussing on network function virtualization and software defined networking. However, a proportionate amount of research is not yet seen in bringing the agility in the physical layer hardware, such as all-optical wavelength conversion which is presently carried out in the electrical domain. When the modulation formats are becoming more complex and superchannel (and flex-grid) systems are being deployed, performing wavelength conversion processes in the electrical layer become extremely inefficient and power consuming because the number of detectors and lasers increases proportionally with the number of subchannels [4]. At the same time, there have been demonstrations of all-optical wavelength conversion in the research laboratories, mostly using nonlinear processes in active and passive media, with four-wave mixing (FWM) being the most attractive technology [5].

We have recently proposed and demonstrated dual-correlated pumping schemes that avoid phase noise transfer from the mixing pumps to the wavelength converted signals (idlers) [6–10]. There have been many studies and demonstrations of the wavelength conversion of polarization

#261322 Received 18 Mar 2016; revised 27 Apr 2016; accepted 12 May 2016; published 20 May 2016

multiplexed and multi-channel signals in nonlinear fibers, [11] being the most recent. In this work, we study the vector theory of dual pump non-degenerate FWM in the nonlinear SOAs and verify the same experimentally for the first time, to the best of our knowledge. We use this to design a polarization insensitive all-optical wavelength converter using FWM and demonstrate the wavelength conversion of single-polarization (SP) and polarization-multiplexed (PM) signals. We demonstrate the wavelength conversion of SP and PM quadrature phase shift keyed (QPSK) and 16-quadrature amplitude modulated (QAM) data at a baud rate of 12.5 GBaud. We extend our investigation to demonstrate the wavelength conversion of four channel Nyquist WDM super-channel PM-QPSK signal, with all the sub-channels operating at a baud rate of 12.5 GBaud.

This paper is organized as follows: in section 2, we discuss the vector theory of FWM in an SOA and provide an experimental validation. In section 3, we use the vector theory of FWM to design an experimental system for the demonstration of polarization insensitive wavelength conversion of PM signals. In section 4, we discuss the results of the wavelength conversion of PM-QPSK, PM-16QAM and four channel Nyquist WDM super-channel, modulated with PM-QPSK signals. We show in appendix A that the use of parallel pumps is preferred over orthogonally polarized pumps for achieving polarization insensitive wavelength conversion of PM signals because it is easier to achieve unitary matrix transformation using parallel pumps.

2. Theory and validation

Consider a non-degenerate FWM process where three frequencies (two pumps and a signal) mix in a nonlinear medium to generate new frequencies (referred to as idlers). The vector representation of the mixing frequencies are shown in Fig. 1(a). We initially consider linearly polarized pumps orthogonal to each other, and a linearly polarized signal at an arbitrary polarization angle with respect to the pumps. The spectral respresentation of such a general FWM scheme is given in Fig. 1(b), showing one of the generated idlers.

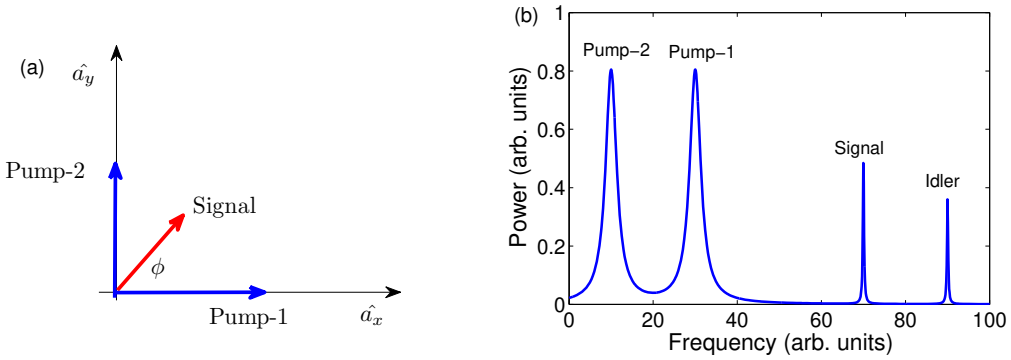

Fig. 1. (a) Vector representation of mixing frequencies, (b) Spectral representation of the mixing frequencies and the generated frequency.

The electric field vectors of the two mixing pumps ($\vec{E}_{p1}$ and $\vec{E}_{p2}$) and the signal ($\vec{E}_{s}$) are given by,

$$\vec{E}_{p1} = A_{p1}\exp(j(\omega_{p1}t - \phi_{p1}))\hat{a_x}, \tag{1}$$

#261322 Received 18 Mar 2016; revised 27 Apr 2016; accepted 12 May 2016; published 20 May 2016

$$\overrightarrow{E}_{p2} = A_{p2}\exp(j(\omega_{p2}t - \phi_{p2}))\hat{a_y}, \tag{2}$$

$$\overrightarrow{E}_{s} = A_s\exp(j(\omega_s t - \phi_s))\left[\cos(\phi)\hat{a_x} + \sin(\phi)\hat{a_y}\right], \tag{3}$$

where A_{p1}, A_{p2} and A_s are the amplitudes, ω_{p1}, ω_{p2} and ω_s are the frequencies, ϕ_{p1}, ϕ_{p2}, ϕ_s are the phases of the pump-1, pump-2 and the signal respectively; ϕ represents the angle between the signal polarization direction and $\hat{a_x}$. Since the polarisation dependent gain of the SOA used is less than 1 dB [12], we assume that the SOA is polarisation independent. Phase noise transfer free wavelength conversion for phase modulated data can be achieved for the idlers corresponding to frequencies $\omega_{p1} - \omega_{p2} + \omega_s$ and $\omega_{p2} - \omega_{p1} + \omega_s$, when the two pumps have correlated phase noise [6]. Of the two idler frequencies, we choose to analyze the polarization preserving properties of idler at frequency $\omega_{p1} - \omega_{p2} + \omega_s$.

The FWM process in an SOA has been explained by the formation of gain gratings and the scattering of one of the mixing frequencies from these gratings [13]. In such a scenario, ω_i under consideration is generated from two gratings formed between, (a) ω_{p1} and ω_{p2} and, (b) ω_s and ω_{p2}. Gain gratings cannot be formed when the mixing frequencies are orthogonally polarized and the strength of the grating is maximum when they are parallelly polarized [10, 13]. Thus the generated idler field can be mathematically expressed as [14–16],

$$\overrightarrow{E}_{i} = \eta_1(\overrightarrow{E}_{p1}.\overrightarrow{E}^{*}_{p2})\overrightarrow{E}_{s} + \eta_2(\overrightarrow{E}_{s}.\overrightarrow{E}^{*}_{p2})\overrightarrow{E}_{p1}, \tag{4}$$

where η_1 and η_2 are the conversion efficiencies of the two processes that represent the strength of the two gratings. The conversion efficiencies are decided by the input power levels of the mixing frequencies and the detuning between them. The dot product of two field vectors ('.') that represents the beating operation, becomes zero when the mixing frequencies are orthogonally polarized to each other and maximum when they are parallelly polarized. Hence for the case described in Fig. 1, the first term in Eq. (4) becomes zero. Substituting Eq. (1), Eq. (2) and Eq. (3) in Eq. (4), the idler field is given by,

$$\overrightarrow{E}_{i} = \eta_2 A_s A_{p1} A^{*}_{p2}\exp(j(\omega_{p1} - \omega_{p2} + \omega_s)t - (\phi_{p1} - \phi_{p2} + \phi_s))\sin(\phi)\hat{a_x}. \tag{5}$$

It is observed that $\overrightarrow{E}_{i}$ is maximum when the angle, ϕ, is 90 degrees, which is when $\overrightarrow{E}_{s}$ is parallel to $\overrightarrow{E}_{p2}$. When ϕ is 0 degrees, the $\overrightarrow{E}_{i}$ becomes minimum because $\overrightarrow{E}_{s}$ is orthogonal to $\overrightarrow{E}_{p2}$ and does not lead to the formation of a grating that scatters the pump, $\overrightarrow{E}_{p1}$, to the frequency ω_i. It can also be observed that the generated idler is parallel to $\overrightarrow{E}_{p1}$, which is along $\hat{a_x}$ direction thereby satisfying the conservation of momentum [17].

2.1. Experimental validation

The experimental setup for validating the theory is given in Fig. 2. Two pump frequencies from an optical frequency comb [18, 19], 120 GHz apart are amplified using an Erbium doped fiber amplifier (EDFA), filtered using two ports in the wavelength selective switch (WSS, waveshaper 4000s) and combined using a polarization beam splitter (PBS). Polarization controllers (PC) are used to maximize the output from the PBS, thereby making the two pumps orthogonally polarized. The orthogonal pumps are then combined with the signal derived from an external cavity laser (ECL) in a 3 dB coupler. The polarization state of the signal is adjusted using a PC to align its polarization with that of the two pumps (one at a time) for the analysis. These three frequencies undergo FWM in the nonlinear SOA (SOA-XN-OEC-1550) and the output is analyzed in an optical spectrum analyzer (OSA). The total input power of the pump wavelengths to the SOA is 0 dBm and the signal power at the input of the SOA is -10 dBm [20].

#261322 Received 18 Mar 2016; revised 27 Apr 2016; accepted 12 May 2016; published 20 May 2016

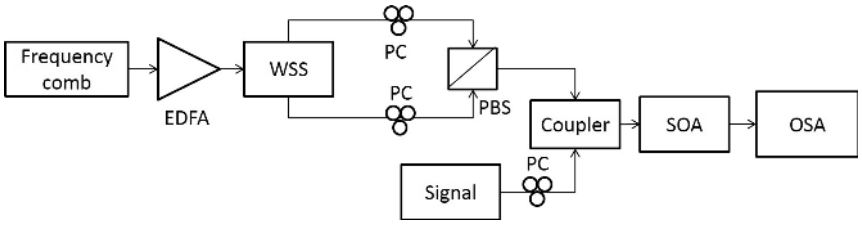

Fig. 2. Schematic of the experimental setup for validating the vector theory of FWM in SOA.

We consider two cases, (a) when the signal is perpendicular to pump-2 ($\phi = 0^0$) and (b) when the signal is parellel to pump-2 ($\phi = 90^0$). The output spectrum corresponding to these cases are shown in Fig. 3(a) and 3(b) respectively. The idlers, pumps and the signal are numbered and marked in the figure.

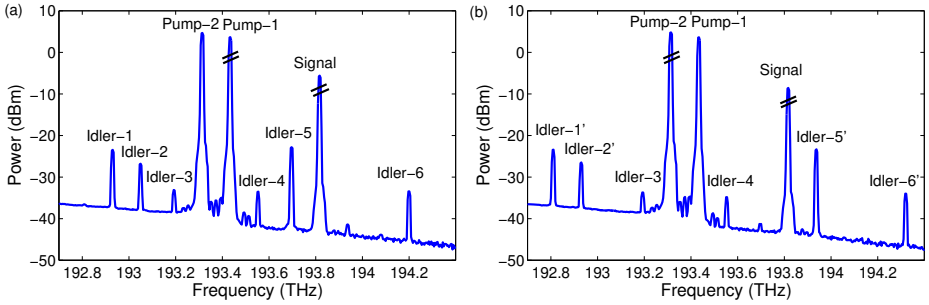

Fig. 3. (Case-a)Spectrum at the output of SOA when the signal polarization is parallel to that of the pump-1, (Case-b)Spectrum at the output of SOA when the signal polarization is parallel to that of the pump-2.

We now analyze the frequencies of the idlers that are generated, use the principle of conservation of energy to understand the mixing processes that generate each idler and list them in Table. 1. The possible frequencies of the idlers produced by the mixing of different frequencies are represented by $\omega_{i1/2/3..}$. The frequencies of the two pumps are, ω_{p2} = 193.315 THz and ω_{p1} = 193.43 THz; while that of the signal is ω_s = 193.82 THz. The idlers generated in our experiments are indicated as ticks and those which are not generated are marked as crosses in the Table 1.

From Fig. 3(a) and 3(b), it can be observed that though the pumps were adjusted to be orthogonal, the frequencies, ω_{i3} and ω_{i4} generated due to the beat between ω_{p1} and ω_{p2}, have non-zero power levels, implying that the two pumps are not completely orthogonal to each other. From Fig. 3(a), Fig. 3(b), Table. 1 and the frequencies of the generated idlers, the following conclusions can be made.

2.1.1. Case-a ($\phi = 0^0$)

- Generation of frequencies of the idlers at ω_{i2} and ω_{i6}, show that signal and the pump-1 are parallel to each other. It can also be inferred that the signal polarization is perpendicular to that of the pump-2 because there are no idlers generated due to the beat between the signal and pump-2.

- It can also be inferred that the idler frequency - ω_{i5}- generated due to the beat between

#261322 Received 18 Mar 2016; revised 27 Apr 2016; accepted 12 May 2016; published 20 May 2016

Table 1. Frequencies of the idlers generated by different FWM processes. The frequencies generated in our experiments for the cases, (a) $\phi = 0^0$ where the signal is co-polarised with the pump1, and (b) $\phi = 90^0$, where the signal is co-polarised with pump-2, are indicated as ticks. The FWM frequencies that are beating to generate a grating are given in red and the frequency that is diffracted by this beat frequency is given in black in column two.

Idler	Mixing frequencies	Frequency (THz)	Case-a ($\phi = 0^0$)	Case-b ($\phi = 90^0$)
ω_{i1}	ω_{p2}+$\omega_{p2} - \omega_{i5}$	192.93	$\surd$	$\times$
ω_{i2}	$\omega_{p1} + \omega_{p1} - \omega_s$	193.05	$\surd$	$\times$
ω_{i3}	$\omega_{p2} + \omega_{p2} - \omega_{p1}$	193.19	$\times$	$\times$
ω_{i4}	$\omega_{p1} + \omega_{p1} - \omega_{p2}$	193.56	$\times$	$\times$
ω_{i5}	$\omega_s - \omega_{p1}$+ω_{p2}	193.7	$\surd$	$\times$
ω_{i6}	$\omega_s + \omega_s - \omega_{p1}$	194.2	$\surd$	$\times$
ω'_{i1}	$\omega_{p2} + \omega_{p2} - \omega_s$	192.81	$\times$	$\surd$
ω'_{i2}	$\omega_{p1} + \omega_{p1} - \omega_{i5}$	192.93	$\times$	$\surd$
ω'_{i5}/ω_i	$\omega_s - \omega_{p2}$+ω_{p1}	193.94	$\times$	$\surd$
ω'_{i6}	ω_s+ $\omega_s - \omega_{p2}$	194.32	$\times$	$\surd$

ω_s and ω_{p1}- is parallel to ω_{p2}. This is because of the generation of ω_{i1}, due to the beat between ω_{i5} and ω_{p2}. Also, no other idler components are generated due to the beat between ω_{i5} and ω_{p1}, thereby validating Eq. (5).

2.1.2. Case-b ($\phi = 90^0$)

To cross-verify, we rotate the polarization of the signal such that it is parallel to pump-2, and analyze the generated idlers.

- Generation of idlers corresponding to frequencies ω'_{i1} and ω'_{i6}, show that signal and the pump-2 are parallel to each other. It can also be inferred that the signal and the pump-1 are orthogonal to each other because there are no idlers generated due to the beat between signal and the pump-1.
- It can be observed that the idler frequency of interest, ω'_{i5} and the pump-1 are parallel to each other, because only the beat between ω_{p1} and ω'_{i5} leads to the generation of the idler at ω'_{i2}.

We analyzed the vector theory for different scenarios and we next show that the use of parallelly polarized pumps are best suited for the polarization insensitive wavelength conversion of PM signals.

2.2. Vector theory for polarization-multiplexed signal

Consider non-degenerate FWM of two pumps and a signal, with the co-polarized pumps, as indicated in Fig. 4(a). The signal consists of two orthogonally polarized fields, which are at an arbitrary angle ϕ, with respect to the pumps, as shown in Fig. 4(a).

The electric field corresponding to the mixing frequencies are given by,

$$\overrightarrow{E}_{p1} = A_{p1}\exp(j(\omega_{p1}t - \phi_{p1}))\hat{a}_x, \tag{6}$$

$$\overrightarrow{E}_{p2} = A_{p2}\exp(j(\omega_{p2}t - \phi_{p2}))\hat{a}_x, \tag{7}$$

#261322 Received 18 Mar 2016; revised 27 Apr 2016; accepted 12 May 2016; published 20 May 2016

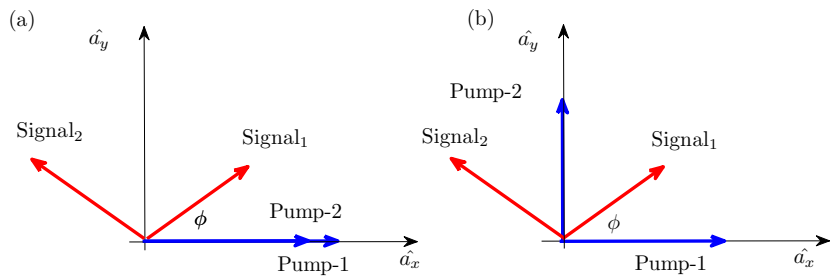

Fig. 4. Vector representation of mixing frequencies when the signal is polarization multiplexed and the pumps are (a) parallelly polarized, (b) orthogonally polarized .

$$\overrightarrow{E}_s = \exp(j(\omega_s t - \phi_s))\,[(A_{s-1}\cos(\phi) + A_{s-2}\cos(90+\phi))]\,\hat{a_x} + \exp(j(\omega_s t - \phi_s))\,[A_{s-1}\sin(\phi) + A_{s-2}\cos(\phi)]\,\hat{a_y}, \tag{8}$$

where A_{s-1} and A_{s-2} represent the amplitudes of the orthogonal components of the signal. We now analyze the idler generated at a frequency of $\omega_i = \omega_{p1} - \omega_{p2} + \omega_s$ given in Eq. (4). There are two FWM processes/beatings occuring here as well, with the FWM beat between the two pumps becoming non-zero because they are parallel to each other. Hence the idler field is given by,

$$\begin{aligned}\overrightarrow{E}_i = {} & A_{p1}A_{p2}^{*}A_s\exp(j(\omega_{p1} - \omega_{p2} + \omega_s)t - (\phi_{p1} - \phi_{p2} + \phi_s))(\eta_1 + \eta_2) \\ & [A_{s-1}\cos(\phi) + A_{s-2}\cos(90+\phi)]\,\hat{a_x} \\ & + \eta_1 A_{p1}A_{p2}^{*}A_s\exp(j(\omega_{p1} - \omega_{p2} + \omega_s)t - (\phi_{p1} - \phi_{p2} + \phi_s)) \\ & [A_{s-1}\sin(\phi) + A_{s-2}\cos(\phi)]\,\hat{a_y}.\end{aligned} \tag{9}$$

When the angle, ϕ, becomes 90 degrees, A_{s-1} component becomes maximum in the $\hat{a_y}$ direction. At the same time, A_{s-2} component becomes maximum in the $\hat{a_x}$ direction. When the angle, ϕ, becomes 0 degrees, A_{s-1} becomes maximum in the $\hat{a_x}$ direction and A_{s-2} becomes maximum in the $\hat{a_y}$ direction. At all other angles, a mix of components of both the polarizations of the signal appear in the $\hat{a_x}$ and $\hat{a_y}$ directions. Representing the electric field of the idler as, $E_i = A_{i-1}\hat{a_x} + A_{i-2}\hat{a_y}$, where A_{i-1} and A_{i-2} are the orthogonal components of the idler and assuming $|\eta_1| >> |\eta_2|$, Eq. (9) can be written as,

$$\begin{bmatrix} A_{i-1} \\ A_{i-2} \end{bmatrix} = \eta_1 A_{p1}A_{p2}^{*}A_s\exp(j(\omega_{p1} - \omega_{p2} + \omega_s)t - (\phi_{p1} - \phi_{p2} + \phi_s)) \begin{bmatrix} \cos(\phi) & -\sin(\phi) \\ \sin(\phi) & \cos(\phi) \end{bmatrix} \begin{bmatrix} A_{s-1} \\ A_{s-2} \end{bmatrix}. \tag{10}$$

It can be observed from Eq. (10) that this matrix transformation is unitary, thus the idler polarizations can always be demultiplexed in the coherent receiver using a polarization-demultiplexing algorithm [21]. If the reference directions for $\hat{a_x}$ and $\hat{a_y}$ are along the directions of A_{s-1} and A_{s-2} respectively, it can be observed that the generated idler components (A_{i-1} and

#261322 Received 18 Mar 2016; revised 27 Apr 2016; accepted 12 May 2016; published 20 May 2016

A_{i-2}) have the same polarizations as that of the signal. The assumption that $|\eta_1| >> |\eta_2|$ is valid because we chose the frequencies of the pumps and the signal such that the detuning between the two pumps are smaller than the detuning between the signal and any of the two pumps [6]. This can be physically interpreted as the beating of two co-polarized pumps thereby creating a gain and refractive index modulation with a frequency corresponding to the detuning between them, which then scatters the data-modulated signal light irrespective of its polarization state. It must be noted that this analysis considers only the FWM process and ignores the distortions such as polarization dependent loss/gain introduced by the nonlinear medium which could result in different η_1 along the orthogonal directions.

The approach outlined in this paper differs from the traditional methods that uses orthogonally polarized pumps to achieve polarization insensitive wavelength conversion [14, 15], vector representation of which is given in Fig. 4(b). We show in the appendix A that it is easier to achieve unitary transformation using parallely polarized pumps rather than orthogonally polarized pumps. The corresponding idler also has phase noise preserving properties [6].

3. Experimental setup for the wavelength conversion of polarization multiplexed signals

The schematic of the experimental setup is given in Fig. 5. Two pumps from two independent lasers are passed through PC, combined using a 3 dB coupler (coupler) and passed through the slow/fast axis of PBS to ensure that both the pumps are parallelly polarized. The co-polarized pumps are then amplified and coupled with a modulated signal and passed through a nonlinear SOA to undergo FWM. The SOA is operated at 500 mA and the total input power of the two pumps are 0 dBm and the input signal power is -10 dBm for the best conversion efficiency [20]. For these operating conditions, we achieve a conversion efficiency (defined as the ratio of output idler power to the input signal power) of $\sim 100\%$ for a detuning of upto 3 nm between the two pumps. The electrical pseudo-random binary sequence (PRBS) signals are generated using an arbitrary waveform generator operating at 25 GSa/s, thereby giving 2 Sa/symbol for signals at 12.5 GBaud. These two electrical PRBS signals are amplified using a radio frequency (RF) amplifier (Amp.) to drive an IQ modulator. The output from the modulator is split and further combined using two PBCs, one arm of which is delayed to emulate PM signals. It is ensured that the two arms of the PM emulator have identical losses. The frequencies of the two pumps, the signal and the wavelength converted idler is similar to Fig. 3. The linewidth of the lasers used as pumps and signals are ~ 100 kHz and a few tens of kHz respectively. The optical channels used for generating the Nyquist WDM superchannel are obtained from a gain-switched laser comb source (GSCS) with a free spectral range (FSR) of 20 GHz and amplified by an EDFA [18, 19]. Matched root raised cosine filters with a roll of factor of 0.1% is used at the transmitter and the receiver in case of Nyquist signaling.

The output from the SOA is filtered for analysis using a bandwidth tunable bandpass filter. The OSNR of the signal/idler is changed by coupling amplified spontaneous emission (ASE) from an EDFA that is passed through a broadband filter (bandwidth of which is 1 nm for single channel signals and 5 nm for Nyquist WDM channels). The signal/idler that is combined with the ASE is then passed to a coupler. One output from the coupler is given to the OSA for analysing the OSNR and the second output is given to the polarization diversity coherent receiver, the input power to which is kept constant. The output of the coherent receiver is given to a real time oscilloscope (RTO) where the signals are captured at 50 GSa/s and analyzed offline. The offline digital signal processing (DSP) includes constant modulus algorithm (CMA) based polarization demultiplexing (multimodulus algorithm (MMA) for multi level 16QAM signals) [21, 22], peridogram based frequency offset estimation [23], decision directed phase noise estimation and training symbol based synchronization [24]. No optical filtering is used for

#261322 Received 18 Mar 2016; revised 27 Apr 2016; accepted 12 May 2016; published 20 May 2016

demodulating the Nyquist WDM channels and they are selected by tuning the local oscillator to the desired sub-channel of the Nyquist super-channel.

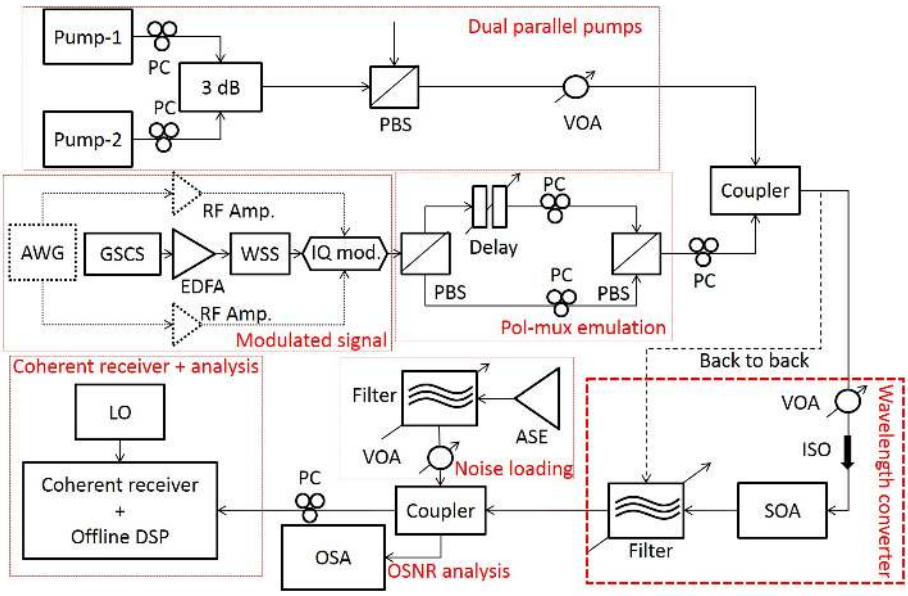

Fig. 5. Schematic of the experimental setup for the demonstration of the wavelength conversion of polarization multiplexed signals.

4. Experimental results

The results of the wavelength conversion of PM-QPSK signals at 12.5 GBaud, with a total bit rate of 50 Gbps are given in Fig. 6. It can be observed from the BER measurements as a function of OSNR (measured at a reference bandwidth of 0.1 nm) that there is no OSNR penalty between the BER values of the input signal (b2b), signal at the SOA output (asoa) and the wavelength converted signal (wc). The OSNR required to obtain a BER of 1e-5 is approximately 17.5 dB for PM-QPSK signals. Although not shown here, the wavelength conversion of SP-QPSK signals is also carried out without any penalty with respect to the BER values of the signal at the input and output of the SOA. In this case, we found that the required OSNR is 15 dB to achieve a BER of 1e-5.

The results of the wavelength conversion of SP and PM-16QAM signals at 12.5 GBaud, with a total bit rate of 50 Gbps and 100 Gps respectively, are given in Fig. 7 and Fig. 8 respectively. It can be observed from the BER measurements as a function of OSNR, measured at a reference bandwidth of 0.1 nm, that there is an OSNR penalty of < 2 dB between the input signal and the signal at the output for BER values lower than 1e-3. This is due to the nonlinear distortions/gain introduced by the SOA. It can be compensated by increasing the pump to signal power ratio, which in-turn will reduce the OSNR of the output wavelength converted signal [25]. There is an additional OSNR penalty of < 2 dB between the the wavelength converted signal and the signal at the output of the SOA also for BER values lower than 1e-3. This is due to the penalty contributions from the signal in addition to the nonlinear distortions introduced by the SOA on the wavelength converted signal. It must be noted that the straight lines in the BER curves are given as a guide to the eye and is not a fit to the data.

The optical spectrum at the input and output of the SOA for the wavelength conversion of

#261322 Received 18 Mar 2016; revised 27 Apr 2016; accepted 12 May 2016; published 20 May 2016

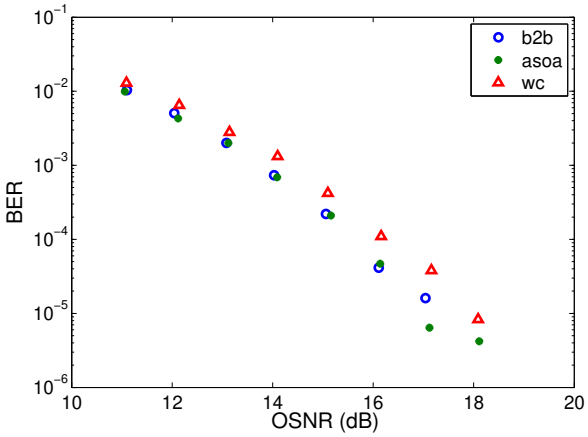

Fig. 6. BER as a function of OSNR for the input signal (b2b), signal after SOA (asoa) and the wavelength converted signal (wc) for polarization-multiplexed QPSK signal at 12.5 GBaud.

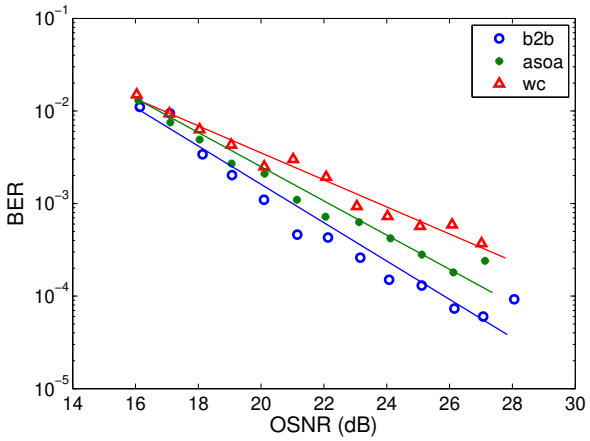

Fig. 7. BER as a function of OSNR for the input signal (b2b), signal after SOA (asoa) and the wavelength converted signal (wc) for single polarization 16-QAM signal at 12.5 GBaud.

12.5 GBaud four channel Nyquist PM-QPSK superchannel are shown in Fig. 9.

The results of the wavelength conversion of the four channel Nyquist WDM super-channel modulated with PM-QPSK signals at 12.5 GBaud, separated by 20 GHz at a total bit rate of 200 Gbps, are given in Fig. 10. As in the case of PM-16QAM data, it is observed from the BER measurements as a function of OSNR, measured at a reference bandwidth of 0.1 nm, that there is a maximum OSNR penalty of < 2 dB between the input signal and the signal at the output for BER values lower than 1e-3. Similarly, there is an additional OSNR penalty of < 2 dB between the wavelength converted signal and the signal at the output of the SOA, for BER values lower than 1e-3. This is believed to be due to the cross-gain modulation effects in the SOA [10].

It must be noted that for these BER measurements, the signal polarization at the input of the SOA was arbitrary. Thus, we have demonstrated polarization insensitive wavelength conversion of single and polarization multiplexed signals. However, there is a penalty incurred

#261322 Received 18 Mar 2016; revised 27 Apr 2016; accepted 12 May 2016; published 20 May 2016

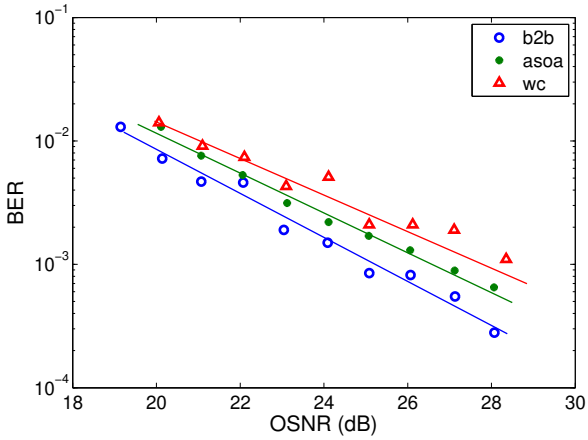

Fig. 8. BER as a function of OSNR for the input signal (b2b), signal after SOA (asoa) and the wavelength converted signal (wc) for polarization-multiplexed 16-QAM signal at 12.5 GBaud.

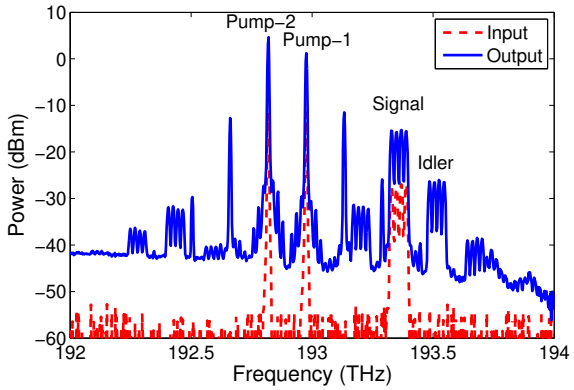

Fig. 9. Optical spectra at the input and output of the SOA for the wavelength conversion of 12.5 GBaud four-channel Nyquist PM-QPSK superchannel.

in the wavelength converted idler which can be mitigated by increasing the pump to signal power ratio, though this increase will lead to a decrease in the conversion efficiency and lower OSNR in the wavelength converted idler. Hence the SOA produces a trade-off between conversion efficiency and the signal quality of the wavelength converted signal, leading to a tighter operating regime with respect to the quality and power levels of the signals input to the SOA [9, 10, 25].

#261322 Received 18 Mar 2016; revised 27 Apr 2016; accepted 12 May 2016; published 20 May 2016

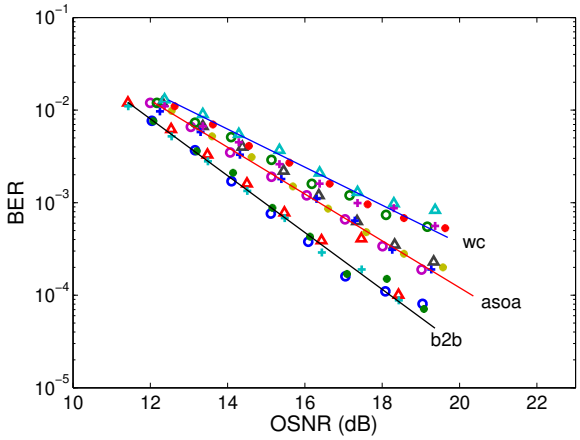

Fig. 10. BER as a function of OSNR for the input signal (b2b), signal after SOA (asoa) and the wavelength converted signal (wc) for four channel Nyquist WDM super-channel modulated with PM-QPSK signals at 12.5 GBaud.

5. Conclusion

We gave the mathematical equations describing the vector theory of four-wave mixing (FWM) in a nonlinear semiconductor optical amplifier (SOA) and experimentally verified them. We demonstrate that by choosing specific idler frequencies, the transfer matrix due to wavelength conversion remains unitary and thus polarization components in the idler can be demultiplexed using the standard polarization demultiplexing algorithms. Utilizing the vector theory of FWM, we proposed and demonstrated a polarization independent scheme for the wavelength conversion of polarization multiplexed signals at 12.5 GBaud without using a polarization diversity system and with two pumps that are co-polarized to each other. We demonstrated the wavelength conversion of single and polarization multiplexed (PM) QPSK and 16QAM signals at 12.5 GBaud with a total bit rates of 25 Gbps (SP-QPSK), 50 Gbps (PM-QPSK), 50 Gbps (SP-16QAM) and 100 Gbps (PM-16QAM) respectively using the proposed scheme. We also demonstrated the wavelength conversion of four channel Nyquist WDM PM-QPSK super-channel at a total bit rate of 200 Gb/s. A maximum OSNR penalty of approximately 3 dB is observed for BER values $<$1e-3 for the wavelength conversion of 16-QAM and PM-QPSK Nyquist WDM channels, between the wavelength converted signal and the input signal to the SOA. This is attributed to the nonlinear gain effects in the SOA. We prove that it is better to use co-polarized dual pumps compared to orthogonally polarized pumps for the all optical wavelength conversion of PM signals using FWM. Even though the vector theory is developed for SOAs, a similar analysis holds good for any nonlinear system that uses four wave mixing for wavelength conversion.

6. Appendix A

Consider a non-degenerate FWM scheme where the orthogonally polarized pumps are mixing with a PM signal, as represented vectorially in Fig. 4(b). The two mixing pumps are given in Eq. (1) and Eq. (2) and the PM signal is represented in Eq. (8). Keeping the notation in section 2, the idler at $\omega_i = \omega_{p1} - \omega_{p2} + \omega_s$ is given by,

$$\overrightarrow{E}_i = \eta_2 (\overrightarrow{E}_s . \overrightarrow{E}^*_{p2}) \overrightarrow{E}_{p1}, \tag{11}$$

#261322 Received 18 Mar 2016; revised 27 Apr 2016; accepted 12 May 2016; published 20 May 2016

$$\overrightarrow{E}_i = \eta_2 A_s A_{p2}^* A_{p1} \exp(j(\omega_{p1} - \omega_{p2} + \omega_s)t - (\phi_{p1} - \phi_{p2} + \phi_s)) \times [A_{s-1}\sin(\phi) + A_{s-2}\cos(\phi)]\,\hat{a_x}. \quad (12)$$

Irrespective of the angle ϕ, the generated idler at $\omega_{p1} - \omega_{p2} + \omega_s$ is polarized along that of the pump-1, i.e along $\hat{a_x}$ in this case. Thus penalty free wavelength conversion of PM data is not possible with orthogonally polarized pumps.

The idler, ω_{i2}, corresponding to frequency $\omega_{p1} + \omega_{p2} - \omega_s$ is usually analyzed for demonstrating polarization insensitivity of FWM/wavelength conversion [14, 15, 26]. This idler is generated by the formation of two gratings and is given by,

$$\overrightarrow{E}_{i2} = \eta_1(\overrightarrow{E}_{p1}.\overrightarrow{E}_s^*)\overrightarrow{E}_{p2} + \eta_2(\overrightarrow{E}_{p2}.\overrightarrow{E}_s^*)\overrightarrow{E}_{p1}, \quad (13)$$

$$\overrightarrow{E}_{i2} = A_{p1}A_{p2}A_s^* \exp(j(\omega_{p1} + \omega_{p2} - \omega_s)t - (\phi_{p1} + \phi_{p2} - \phi_s)) \times [\eta_1(A_{s-1}\cos(\phi) + A_{s-2}\cos(90+\phi))\hat{a_x} + \eta_2(A_{s-1}\sin(\phi) + A_{s-2}\cos(\phi))\hat{a_y}]. \quad (14)$$

From Eq. (14), the orthogonal components of the idlers is given by,

$$\begin{bmatrix} A_{i-1} \\ A_{i-2} \end{bmatrix} = \eta_1 A_{p1} A_{p2} A_s^* \exp(j(\omega_{p1} + \omega_{p2} - \omega_s)t - (\phi_{p1} + \phi_{p2} - \phi_s)) \begin{bmatrix} \eta_1\cos(\phi) & -\eta_1\sin(\phi) \\ \eta_2\sin(\phi) & \eta_2\cos(\phi) \end{bmatrix} \begin{bmatrix} A_{s-1} \\ A_{s-2} \end{bmatrix}, \quad (15)$$

It can be observed from the Eq. (14) that this idler generated at $\omega_{i2} = \omega_{p1} + \omega_{p2} - \omega_s$ is polarization insensitive to a degree and can be used for the wavelength conversion of PM signals since the signal components are getting wavelength converted to both the idler components simultaneously (which does not happen for ω_i in Eq. (12)). However, the matrix transformation in Eq. (15) is not unitary in general and becomes unitary only when $\eta_1 = \eta_2$ which happens in single pump scenarios. Hence demultiplexing them at the receiver will be difficult. Another disadvantage of using this idler is that there will be a phase noise transfer to this idler from the two pumps [6].

Acknowledgments

This work was supported by the EU Project "BIGPIPES", and by the SFI CTVR (10/CE/I1853), CONNECT (13/RC/2077) and IPIC (12/RC/2276) projects. People Programme (Marie Curie Actions) of the European Unions Seventh Framework Programme FP7/2007-2013/ under REA (318941) is thankfully acknowledged.

#261322 Received 18 Mar 2016; revised 27 Apr 2016; accepted 12 May 2016; published 20 May 2016